Transition Met Chem (2010) 35:165–175
DOI 10.1007/s11243-009-9310-0

Studies on the coordination chemistry of methylated xanthines and their imidazolium salts. Part 1: benzyl derivatives

Vanessa R. Landaeta · Rafael E. Rodríguez-Lugo · Eloy N. Rodríguez-Arias · David S. Coll-Gómez · Teresa González

Received: 1 September 2009 / Accepted: 9 November 2009 / Published online: 24 November 2009

Abstract New imidazolium salts derived from the natural methylated xanthines theophylline, theobromine and caffeine, namely 1,3-dimethyl-9-benzylxanthinium bromide (tphBzBr, **1a**), 3,7-dimethyl-9-benzylxanthinium bromide (tbrBzBr, **2a**) and 1,3,7-trimethyl-9-benzylxanthinium bromide (caffBzBr, **3a**), are reported. Also, the disubstituted analog of **1a**, 1,3-dimethyl-7,9-dibenzylxanthinium bromide (tphBz$_2$Br, **1a**′) was identified and characterized by NMR. The coordination chemistry of ligands **1a**–**3a** toward palladium, and some theoretical aspects of the unmodified theophylline, theobromine and caffeine are studied. Our results prove that the theophylline derivative has the thermodynamic tendency to form N-bonded species, even when an equilibrium between the Pd–NHC and the "theophyllinate" was observed spectroscopically, due to the anisotropy of the NHC ligand. To confirm the N-coordination, the solid state structure of the new "theophyllinate" species PdBr$_2$(tphBz-H)$_2$ (**4**), derived from **1a**, was determined by X-ray diffraction. The analog with theobromine, ligand **2a**, coordinates to palladium via N1, in an analogous manner to **1a**, and a mixture of the cis/trans isomers of its palladium complex is obtained. On the other hand, since there is no possibility of N-coordination in **3a**, this caffeine derivative forms a Pd-NHC compound after deprotonation with a strong base. Both the theoretical results and the experimental evidence are in accordance, in terms of the predicted coordination sites or possibility of modification of the selected methylated xanthines to obtain new ligands.

Electronic supplementary material The online version of this article (doi:10.1007/s11243-009-9310-0) contains supplementary material, which is available to authorized users.

V. R. Landaeta (✉) · R. E. Rodríguez-Lugo · E. N. Rodríguez-Arias
Departamento de Química, Universidad Simón Bolívar, Valle de Sartenejas, Baruta. Apartado 89000, Caracas 1080, Venezuela
e-mail: vlandaeta@usb.ve

Present Address:
R. E. Rodríguez-Lugo
Laboratory for Inorganic Chemistry, Swiss Federal Institute of Technology, ETH Zurich, HCI-H136 Zürich, Switzerland

D. S. Coll-Gómez
Centro de Química, Laboratorio de Química Computacional, Instituto Venezolano de Investigaciones Científicas, IVIC, Caracas, Venezuela

T. González
Centro de Química, Laboratorio Nacional de Difracción de Rayos X, Instituto Venezolano de Investigaciones Científicas, IVIC, Caracas, Venezuela

Introduction

The natural methylated xanthines, theophylline, theobromine and caffeine (Fig. 1) are found in tea, cocoa and coffee. They exhibit biologic activity [1] as stimulants, and they have also been used for pharmacologic purposes [2]. In this sense, several efforts have been made to study their coordination chemistry toward "essential metals" [3] and their interaction with transition metals [3–8]. For instance, Williams [2] et al. reported an analog to cis-platin with caffeine, Pt(caff)$_2$Cl$_2$, and there are reports in which the thermal behavior of these xanthines under physiological conditions has been studied [3–6]. Also, Taube and coworkers [7] proposed a C(8) coordination to ruthenium in the unmodified caffeine and theobromine ligands, and a mixed N–C, coordination fashion in theophylline.

However, there are only a few reports of inorganic compounds with functionalized xanthines [9]. Among

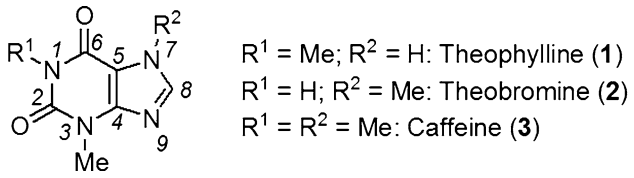

Fig. 1 Chemical structure of the selected natural methylated xanthines

them, 8-alkyl-derivatives from theophylline [9] and N-methyl caffeine [10–13] have been reported. To the best of our knowledge, none of those exist with C(8) or N(9)-substituted modified theobromine.

On the other hand, even when natural methylated xanthines have an azole ring and a bulky backbone attached to it [14], which makes them potentially interesting to prepare N-Heterocyclic Carbenes (NHC's) and their complexes (for selected references on some of the most recent advances in the chemistry of NHC's ligands, see [15–19]), those only exist with N-methyl caffeine, and examples of its coordination chemistry are found exclusively with mercury [20], silver [10], iridium and rhodium [10, 13]. The first 1,3,7,9-tetramethylxanthine-8-ylidene complex was reported as a mercury bis-carbene complex [20]. Youngs et al. prepared a silver (I) bis-carbene complex, which has been evaluated as antimicrobial agent, and a cationic rhodium (I) complex [10, 11]. Herrmann and coworkers also obtained rhodium (I) and iridium (I) carbene complexes of the type $[M(L)(L_{Carbene})_2]I$ and $M(L)(L_{Carbene})(I)$ (M = Rh, Ir, $L_{Carbene}$ = 1,3,7,9-tetramethylxanthine-8-ylidene, 7,9-dimethylhypoxanthine-8-ylidene, L = η^4-1,5-cyclooctadiene = COD) [13]. To date, to the best of our knowledge, no NHC's have ever been reported with the modified theophylline or theobromine.

The lack of results with the latter two, and the few reports found in the case of caffeine are then interesting. The difference among them could lie in the fact that caffeine, having three of its nitrogen atoms blocked by methyl groups, is the best candidate to become an NHC precursor. In contrast, the other two xanthines have an acidic proton that could compete with C(8) binding either in the modified or unmodified molecule [7], specially if a base is used to generate the carbene [21].

In this sense, three new imidazolium salts from theophylline (**1**), theobromine (**2**) and caffeine (**3**) bearing the benzyl group on N(9) are reported, as a part of a wider synthetic study. Also, the coordination chemistry of the xanthine derivatives toward palladium(II) was investigated and contrasted with their unmodified counterparts [2–8], determining if the N(1,7) or C(8) hapticity is favored. In addition, a theoretical study of the acidity-basicity and orbital energies of each xanthine, **1**-**3**, was performed, observing a match between theoretical results and the experimental evidence in the modification of these methylated xanthines and their coordination chemistry toward palladium.

Experimental

All reactions and manipulations were routinely performed under dry nitrogen or argon atmosphere using standard Schlenk techniques. ^{1}H, and ^{13}C{^{1}H} NMR spectra were recorded on a Jeol Eclipse 400 spectrometer (400.13 and 100.5 MHz). Peak positions are relative to tetramethylsilane and were calibrated against the residual solvent resonance (^{1}H) or the deuterated solvent multiplet (^{13}C). All the NMR spectra were recorded at room temperature (25 °C) unless otherwise stated. Infrared spectra were recorded by Bruker IR 560 FT-IR spectrometer, using samples mulled in Nujol between KBr plates or in KBr disks. HRMS analyses were performed using a Bruker Daltonics maxis ESI-QTOF and a Varian HiResMALDI by ETH Zürich DCHAB/LOC MS-Service. X-ray diffraction studies were performed on a Rigaku AFC-7S diffractometer with a Bruker Smart Apex area detector by the X-ray diffraction service of Laboratorio Nacional de Difracción de Rayos X at IVIC.

Unless otherwise stated, all solvents were distilled just prior to use from appropriate drying agents. Dichloromethane was distilled from CaH_2, and tetrahydrofuran (THF) from sodium/benzophenone. Diethylether and petroleum ether were dried with sodium. Deuterated solvents were dried over 4-Å molecular sieves prior to use. All other chemicals were commercial products and used as received without further purification. Literature methods were employed for the synthesis of $(PhCN)_2PdCl_2$ [22].

Synthesis

1,3-Dimethyl-9-benzylxanthinium bromide, or theophyllineBzBr (tphBzBr, ***1a****)*

Theophylline (**1**, 3.00 g, 16.7 mmol) and KI (150 mg, 0.90 mmol) were suspended in acetonitrile (50 mL) and vigorously stirred. After stirring for 5 min, benzyl bromide (8.0 mL, 66.8 mmol) was added. The mixture was refluxed for 4 days. After completion, the crude was cooled and filtered to eliminate any unreacted theophylline and the excess of KI. The solution was evaporated to dryness, and diethyl ether (50 mL) was added. Upon stirring overnight and filtering, white-off needles were obtained. Yield: 3.65 g, 63%. ^{1}H NMR ($CDCl_3$, 25 °C, 400.13 MHz): δ 3.35 (s, 3H, CH_3–N); δ 3.53 (s, 3H, CH_3–N); δ 5.45 (s, 2H, PhCH_2–N); δ 7.31–7.29 (m, 5H, aromatics); δ 7.56 (s, 1H, C–*H*). ^{13}C{^{1}H} NMR ($CDCl_3$, 25 °C, 100.5 MHz): δ 28 (*C*H_3–N); δ 30 (*C*H_3–N); δ 50 (Ph*C*H_2–N); δ 107 (O=C–

C–N); δ 128 (aromatic, *para*); δ 128.7 (aromatic, *meta*); δ 129 (aromatic, *ortho*); δ 135 (*C ipso*); δ 141 (N–*C*H=N); δ 149 (N–*C*–N); δ 151 (N–*C*(=O)–N); δ 155 (N–*C*(=O)–C). HRMS (ESI): m/z calcd for $C_{14}H_{15}N_4O_2Br$: 271.1195 [M^+–Br]; found 271.1185. FT-IR υ (cm^{-1}): 1701 (C=O), 1655 (C=O).

*Characterization of 1,3-dimethyl-9,7-dibenzylxanthinium bromide (tphBz$_2$Br, **1a′**)*

^{1}H NMR ($CDCl_3$, 25 °C, 400.13 MHz): δ 3.40 (s, 3H, C*H*$_3$–N); δ 3.58 (s, 3H, C*H*$_3$–N); δ 5.54 (s, 4H, PhC*H*$_2$–N); δ 7.30–7.45 (m, 10H, aromatics); δ 7.58 (s, 1H, C–*H*). HRMS (ESI): m/z calcd for $C_{21}H_{21}N_4O_2Br$: 361.1664 [M^+–Br]; found 361.1655.

*3,7-Dimethyl-9-benzylxanthinium bromide, or theobromineBzBr (tbrBzBr, **2a**)*

Theobromine (**2**, 0.50 g, 2.80 mmol) and KI (23 mg, 0.14 mmol) were suspended in benzyl bromide (5 mL) and vigorously stirred. The mixture was refluxed for 24 h, cooled and filtered to eliminate any unreacted xanthine and KI. Diethyl ether (10 mL) was added and upon stirring overnight and filtering, a brown powder was obtained. Yield: 0.94 g, 96%. ^{1}H NMR (DMSO-d_6, 80 °C, 400.13 MHz): δ 3.35 (s, 3H, C*H*$_3$–N); δ 3.86 (s, 3H, C*H*$_3$–N); δ 5.46 (s, 2H, PhC*H*$_2$–N); δ 7.33–7.02 (m, 5H, aromatics); δ 7.90 (s, 1H, C–*H*); δ 10.72 (broad, 1H, N–*H*). ^{13}C{^{1}H} NMR (DMSO-d_6, 80 °C, 100.5 MHz): δ 29 (*C*H$_3$–N); δ 34 (*C*H$_3$–N); δ 50 (Ph*C*H$_2$–N); δ 108 (O=C–*C*–N); δ 128.1 (aromatic, *para*); δ 128.4 (aromatic, *meta*); δ 129 (aromatic, *ortho*); δ 135 (*C ipso*); δ 143 (N–*C*H=N); δ 150 (N–*C*–N); δ 152 (N–*C*(=O)–N); δ 155 (N–*C*(=O)–C). HRMS (MALDI-FT): m/z calcd for $C_{14}H_{15}N_4O_2Br$: 350.0378 [M]; found 350.0435. FT-IR υ (cm^{-1}): 1685 (C=O).

*1,3,7-Trimethyl-9-benzylxanthinium bromide, or caffeineBzBr (caffBzBr, **3a**)*

Caffeine (**3**, 1.00 g, 5.15 mmol) was suspended in benzyl bromide (10 mL) and vigorously stirred. The mixture was refluxed for 24 h and then cooled and filtered to eliminate any unreacted **3**. The solvent was reduced under vacuum, and diethyl ether (50 mL) was added. Upon stirring for 1 h and filtering, a pale brown powder was obtained. Yield: 0.81 g, 43%. ^{1}H NMR ($CDCl_3$, 25 °C, 400.13 MHz): δ 3.39 (s, 3H, C*H*$_3$–N); δ 3.57 (s, 3H, C*H*$_3$–N); δ 3.98 (s, 3H, C*H*$_3$–N); δ 5.49 (s, 2H, PhC*H*$_2$–N); δ 7.34–7.30 (m, 5H, aromatics); δ 7.58 (s, 1H, C–*H*). ^{13}C{^{1}H} NMR ($CDCl_3$, 25 °C, 100.5 MHz): δ 28 (*C*H$_3$–N); δ 30 (*C*H$_3$–N); δ 33 (*C*H$_3$–N); δ 50 (Ph*C*H$_2$–N); δ 107 (O=C–*C*–N); δ 128 (aromatic, *para*); δ 128.5 (aromatic, *meta*); δ 129 (aromatic, *ortho*); δ 135 (*C ipso*); δ 141 (N–*C*H=N); δ 149 (N–*C*–N); δ 151 (N–*C*(=O)–N); δ 155 (N–*C*(=O)–C). HRMS (ESI): m/z calcd for $C_{15}H_{17}N_4O_2Br$: 285.1351 [M^+–Br]; found: 285.1346. FT-IR υ (cm^{-1}): 1698 (C=O), 1649 (C=O).

*trans-Dibromo bis-7-(1,3-dimethyl-9-benzylxanthine) palladium(II) (**4**)*

1,3-dimethyl-9-benzylxanthinium bromide (**1a**, 600 mg, 1.71 mmol) was dissolved in acetonitrile (10 mL). Palladium acetate (190 mg, 0.86 mmol) and sodium bromide (176 mg, 1.71 mmol) were added, and the mixture was refluxed for 24 h, cooled and filtered to eliminate the excess of NaBr and any unreacted **1a**. The yellow solution was evaporated to dryness. Yield: 370 mg, 54%. ^{1}H NMR ($CDCl_3$, 25 °C, 400.13 MHz): δ 3.46 (s, 1H, C*H*$_3$–N); δ 3.60 (s, 1H, C*H*$_3$–N); δ 4.57 (s, 3H, C*H*$_3$–N); δ 4.72 (s, 3H, C*H*$_3$–N); δ 5.54 (s, 2H, PhC*H*$_2$–N); δ 5.57 (s, 2H, PhC*H*$_2$–N); δ 7.41–7.33 (m, 10H, aromatics); δ 7.91 (s, 1H, C–*H*); 8,00 (s, 1H, C–*H*). ^{13}C{^{1}H} NMR ($CDCl_3$, 25 °C, 100.5 MHz): δ 28.5 (*C*H$_3$–N); δ 30 (*C*H$_3$–N); δ 33 (*C*H$_3$–N); δ 33.4 (*C*H$_3$–N); δ 51.7 (Ph*C*H$_2$–N); δ 51.8 (Ph*C*H$_2$–N); δ 108.3 (O=C–*C*–N); δ 108.4 (O=C–*C*–N); δ 128.2; δ 128.5; δ 129.4; δ 129.5; δ 129.6 (aromatics); δ 133 (*C ipso*); δ 133.2 (*C ipso*); δ 140 (N–*C*H=N); δ 146.7 (N–*C*–N); δ 146.9 (N–*C*–N); δ 150.9 (N–*C*(=O)–N); δ 151 (N–*C*(=O)–N); δ 153.9 (N–*C*(=O)–C); δ 154.1 (N–*C*(=O)–C).

*trans-Dichloro bis(1,3,7-trimethyl-9-benzylxanthine-8-ylidene) palladium(II) (**6**)*

1,3,7-trimethyl-9-benzylxanthinium bromide (**3a**, 91 mg, 0.25 mmol) was suspended in THF (1.5 mL), and a solution of potassium tertbutoxide (28 mg, 0.25 mmol) in THF (0.5 mL) was slowly added at room temperature. The mixture was stirred at room temperature for 3 h and filtered to eliminate KBr, and a brown solution was obtained. $PdCl_2(NCPh)_2$ (34 mg, 0.13 mmol) dissolved in acetonitrile (2 mL) was slowly added to the free carbene obtained from **3a** (the brown solution), and the mixture was stirred for 4 h at room temperature. The bright yellow solution was evaporated to dryness Yield: 160 mg, 86%. ^{1}H NMR ($CDCl_3$,, 25 °C, 400.13 MHz): δ 3.36 (s, 3H, C*H*$_3$–N); δ 3.55 (s, 3H, C*H*$_3$–N); δ 3.97 (s, 3H, C*H*$_3$–N); δ 5.52 (s, 2H, PhC*H*$_2$–N); δ 7.37–7.35 (m, 3H, aromatics); δ 7.52 (s, 1H, aromatic, *ortho*); δ 7.63 (s, 1H, aromatic, *ortho*). ^{13}C{^{1}H} NMR ($CDCl_3$, 25 °C, 100.5 MHz): δ 27.5 (*C*H$_3$–N); δ 27.6 (*C*H$_3$–N); δ 29 (*C*H$_3$–N); δ 33 (*C*H$_3$–N); δ 50 (Ph*C*H$_2$–N); δ 107 (O=C–*C*–N); δ 128 (aromatic, *para*); δ 128.3 (aromatic, *meta*); δ 129 (aromatic, *ortho*); δ 135.9 (*C ipso*); δ 136.0 (*C ipso*); δ 141 (N–*C*H=N); δ 141.4 (N–*C*H=N); δ

148.7 (N–*C*–N); δ 148.9 (N–*C*–N); δ 151 (N–*C*(=O)–N); δ 155.2 (N–*C*(=O)–C); δ 155.3 (N–*C*(=O)–C). HRMS (ESI): m/z calcd for $C_{30}H_{32}N_8O_4Cl_2Pd$: 705.1291 [M^+–Cl]; found: 705.2322.

In situ reaction of ***2a*** *with Pd(OAc)₂: Cis and trans-dibromo bis-1-(3,7-dimethyl-9-benzylxanthine) palladium(II) (****5****)*

3,7-dimethyl-9-benzylxanthinium bromide (**2a**, 200 mg, 0.570 mmol) was suspended in acetonitrile (20 mL). Palladium acetate (63.1 mg, 0.281 mmol) and sodium bromide (58 mg, 0.560 mmol) were added. The mixture was refluxed for 24 h, cooled and filtered to eliminate NaBr and any unreacted **2a**. The orange solution was evaporated to dryness. Isomers ratio = 2:1. ^{1}H NMR ($(CD_3)_2CO$, 25 °C, 400.13 MHz): δ 3.42 (s, 3H, C*H*$_3$–N, *trans*); δ 3.43 (s, 3H, C*H*$_3$–N, *trans*); δ 3.91 (s, 3H, C*H*$_3$–N, *cis*); δ 3.97 (s, 3H, C*H*$_3$–N, *cis*); δ 4.70 (s, 2H, PhC*H*$_2$–N, *cis*); δ 5.56 (s, 2H, PhC*H*$_2$–N, *trans*); δ 7.33–7.31 (m, 5H, aromatics, *cis*); δ 7.35–7.33 (m, 5H, aromatics, *trans*); δ 7.94 (s, 1H, C–*H*, *cis*); 8,12 (s, 1H, C–*H*, *trans*). 13C{1H} NMR ($(CD_3)_2CO$, 25 °C, 100.5 MHz): δ 25 (*C*H$_3$–N); δ 30 (*C*H$_3$–N); δ 50 (Ph*C*H$_2$–N); δ 110 (O=C–*C*–N); δ 128.0 (aromatic, *para*); δ 128.2 (aromatic, *meta*); δ 128.8 (aromatic, *ortho*); δ 137 (*C ipso*); δ 142 (N–*C*H=N); δ 150 (N–*C*–N); δ 151 (N–*C*(=O)–N); δ 155 (N–*C*(=O)–C). Both isomers have almost identical ^{13}C{^{1}H} NMR spectra.

*X-ray crystal structure determination for compound (****4****)*

Data for compound **4** was collected using a Rigaku AFC-7S diffractometer, provided with graphite monochromated Mo Kα radiation (λ = 0.71073 Å). Details of the crystal data and structure refinement are shown in Table 1. A semi-empirical absorption correction [23] was applied to the set of data. Crystal structure was solved by direct methods, and the final models were reached by Fourier techniques. All e.s.d.'s (except the e.s.d. in the dihedral angle between two l.s. planes) are estimated using the full covariance matrix. The cell e.s.d.'s are taken into account individually in the estimation of e.s.d.'s in distances, angles and torsion angles; correlations between e.s.d.'s in cell parameters are only used when they are defined by crystal symmetry. An approximate (isotropic) treatment of cell e.s.d.'s is used for estimating e.s.d.'s involving l.s. planes. Refinement of F^2 against ALL reflections. The weighted *R*-factor *wR* and goodness of fit *S* are based on F^2, conventional *R*-factors *R* are based on *F*, with *F* set to zero for negative F^2. The threshold expression of $F^2 > \sigma(F^2)$ is used only for calculating *R*-factors(gt) etc. and is not relevant to the choice of reflections for refinement. *R*-factors based on F^2 are statistically about twice as large as those based on *F*, and *R*-factors based on ALL data will be even larger. All structure solutions and refinements were made using *SHELXS97* [24] and *SHELXL97* [24].

Table 1 Summary of crystal data for $PdBr_2$(tphBz-H)$_2$ (**4**)

	4
Formula	$C_{28}H_{28}Br_2N_8O_4Pd$
Mol. wt.	806.79
Cryst size (mm)	0.50 × 0.45 × 0.10
Cryst. syst.	Monoclinic
Space group	$P2_1/a$
A (Å)	8.308 (3)
B (Å)	11.266 (3)
C (Å)	16.358 (5)
β (°)	93.818 (10)
V (Å^3)	1527.6 (8)
Z	2
d_{calc} (mg/m^3)	1.624
Abs. coeff. (mm^{-1})	3.26
F(000)	736
θ range (°)	2.2–28.0
Index ranges	$-10 \le h \le 9$, $-14 \le k \le 14$, $-18 \le l \le 18$
Tot. no. of data	16898
No. of unique data,	2151
$I \ge 2\sigma(I)$	[*R*(int)] = 0.059
R (all data)	0.0772
	wR = 0.2410
Largest diff. peak and hole (e/Å^3)	0.99, −1.06

Crystallographic data for **4** has been deposited with the Cambridge Crystallographic Data Centre as number CCDC 745624. It contains the supplementary crystallographic data for this paper. These data can be obtained free of charge from The Cambridge Crystallographic Data Centre via www.ccdc.cam.ac.uk/data_request/cif.

Theoretical studies on theophylline (**1**), theobromine (**2**) and caffeine (**3**)

Nature of active sites can be particularly explored using the electrostatic potential, $V(\mathbf{r})$, which let us directly to determine where the electron-rich sites in a molecule or crystal are localized [25–42]. For the region nearest to the nucleus, V_N dominates and $V(\boldsymbol{r})$ has similar topology to the electron density [43, 44], ρ(r). i.e., positive-valued maxima at the nuclear site and a positive-valued saddle point between every pair of bonded atoms. Nevertheless, the existence of maxima is ruled out via an established result that, barring the nuclear position, there cannot exist any strict local maxima in the $V(\boldsymbol{r})$ map [31–33]. For the region where V_E

dominates ($V(\boldsymbol{r})$ is negative) the $V(\boldsymbol{r})$, topography can be more complex. The minima of the negative region denote the zones to which an approaching electrophile may be attracted. On the contrary, the positive regions do not have maxima, which might indicate sites for nucleophilic attack. Nevertheless, Politzer and Sjoberg have shown that by computing $V(\mathbf{r})$ on the 0.002-electron/bohr^3 contour isosurface [45] of the molecular electronic density $\rho(\boldsymbol{r})$, we can quantify the susceptibility of molecules to nucleophilic attack. They demonstrated that relative magnitudes of the positive electrostatic potential in various regions on this surface do reveal the sites most susceptible to nucleophilic attack. Mapping on this isosurface the $V(\boldsymbol{r})$ values onto colors allows us to identify the host sites in which nucleophiles (most positive zone) and electrophiles (most negative zone) should bind. Additionally, the active sites' susceptibility can be quantified determining the minimum and maximum $V(\mathbf{r})$ values at the determined host zones using a Newton–Raphson technique similar to those that have been previously reported by Aray et al. for the study of the electronic density [46, 47] and electrostatic potential topology [40–42, 48].

DMol^3 program [49, 50] was used to calculate $\rho(\boldsymbol{r})$ and $V(\mathbf{r})$. DMol^3 calculates variational self-consistent solutions to the DFT equations, expressed in an accurate numerical atomic orbital basis. The solutions to these equations provide the molecular electron densities, which can be used to evaluate the total electrostatic potential of the system. The correlation and exchange effects were considered using the gradient generalized approximation (GGA) and the functional PW91 [51]. The numerical double-zeta plus polarization basis set DNP was used in all calculations.

Results and discussion

Theoretical modeling on theophylline (**1**), theobromine (**2**) and caffeine (**3**)

Computational calculations on other oxopurines have previously been done. For examples on calculations on oxopurines, see [52–57]. For example, the determination of relevant lowest energy reaction channels in guanine has been studied using ab initio methods [53] and the acid/base behavior of purine analogs was reported, on the basis of theoretical and spectroscopic NMR data [55, 57]. Molecular orbital aspects regarding caffeine have only been considered in terms of its adsorption onto polymeric resins [58].

Figure 2 shows the representation of V(r) over a density isosurface for theophylline (**1**), theobromine (**2**) and caffeine (**3**). The negative zones are represented by the different tones of blue and green, and are located around the oxygen atoms, and N(9) (see Fig. 1 for numbering), in each case. The highest contribution of the electronic distribution is over the oxygen atoms non-bonded electronic pairs, as well as the nitrogen lone pairs in N(9). The basic nature of N(9) in each case becomes then evident. Reported studies show that, for example, for the purine analog guanine and its tautomers, the protons on N(7) and N(9) are the most acidic ones, which reveals the basic nature of the nitrogen atoms in these cases [59], and is also consistent with our results.

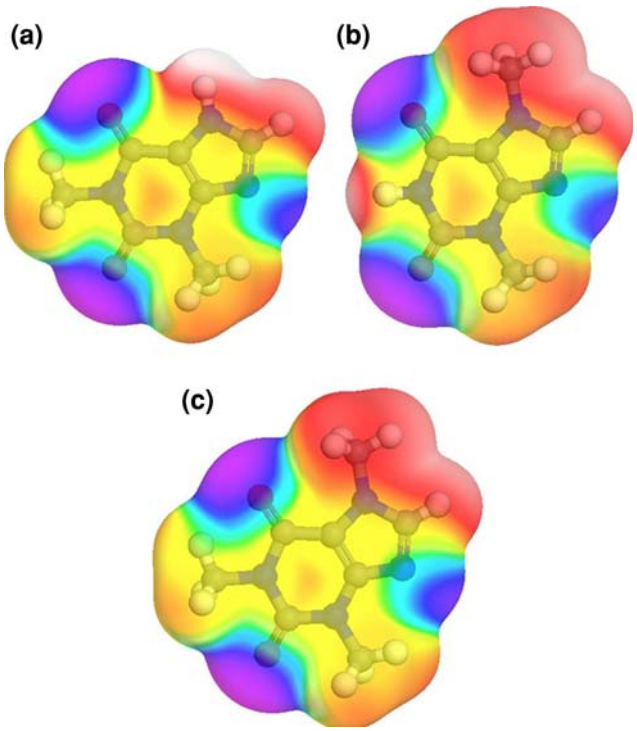

Fig. 2 Methylated xanthines with their representation of V(r). **a** Theophilline, **b** Theobromine, **c** Caffeine. The white spheres correspond to the H atoms, the red ones to the O atom, the blue ones to the nitrogen atoms and the gray ones to the C atoms

The positive sectors are represented with colors between yellow and red. As can be seen from the figure, the most positive zones are located over the groups on C(8) and N(7) in each of the studied xanthines, meaning that these correspond to the most acidic protons in **1**, **2** and **3**.

Theobromine (**2**), in particular, also presents an important center of acidity on the proton bonded to N(1). In the case of theophylline (**1**), the protons from both the C(8) and N(7) centers are mainly acidic. This contrasts with the previously reported data for adenine and guanine [59] in which the C(8) site was much less acidic than N(1), and explains why N(1) in theobromine is highly acidic. The acid/base nature of the centers in these molecules must then become the driving force for any reaction in which they are involved.

In terms of the coordination chemistry of these molecules, it might then be possible to expect their interaction with transition metals to occur mainly through N(9) in each case. For **1** and **2**, the presence of a base in the reaction media might then cause a deprotonation to occur, and the interaction with N(7) for theophylline and N(1) for theobromine should then become possible. Theoretical calculations have been widely considered to predict the reactivity of N-ligands toward metals [60].

One of our objectives was to study the coordination chemistry of the unmodified xanthines **1**, **2** and **3** toward substitution on N(9) in order to obtain new imidazolium salts derived from methylated xanthines. Then, the main objective was to study the coordination chemistry of the new ligands obtained toward palladium, in an attempt to synthesize NHC-Pd compounds, and contrast their behavior with the previously known examples of methylated xanthines-palladium species [2–8].

In this sense, the acid/base analysis of our theoretical results indicates that the unmodified xanthines should interact with transition metals mainly through N(9), which is exactly the position where the modification will be introduced to obtain imidazolium salts. It is important then to study the frontier orbitals of **1**, **2** and **3** to determine, on the orbital level, whether the modification is possible.

The representation of the frontier orbitals of caffeine (**3**) is shown in Fig. 3. Analog representations have been obtained for the frontier orbitals of **1** and **2**, and the figures are available as supplementary material. According to Fig. 3, and also for molecules **1** and **2**, in all cases the Lewis basic site (HOMO) is located in the six-membered ring. Theophylline (**1**) and caffeine (**3**) have essentially the same frontier orbitals, as is expected since both of their six-membered rings are identical. For theobromine (**2**), the geometry of the HOMO is slightly different, probably in response to the presence of a hydrogen atom on N(1), whose electronic effect is different from that of the methyl group. For all of the xanthines, a rich electronic density region is observed on one of the carbonyl groups (C(6)=O) and N(3).

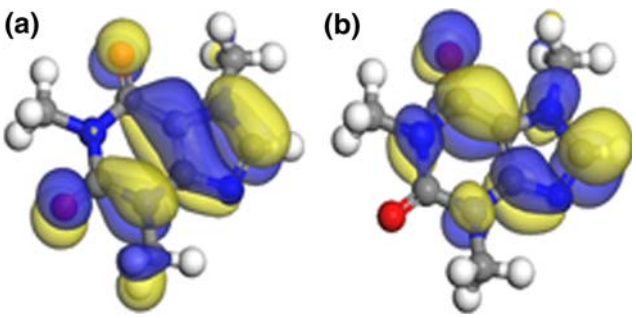

Fig. 3 Representation of the frontier orbitals for caffeine (**3**). **a** HOMO for **3**; **b** LUMO for **3**

On the other hand, the Lewis acid site (LUMO) corresponds to the azole ring, basically around N(7). This might be due to a partial delocalization of the electron lone pair in the five-membered ring. The acidic character is actually remarkable when the substituent on N(7) is a proton (theophylline, **1**). This prediction of our model totally agrees with the experimental observations that have previously been reported [3, 9], where theophylline can be easily deprotonated in presence of a basic late transition metal precursor or a late transition metal precursor in basic conditions, yielding N(7) coordinated species. The preferential coordination site at N(7), which has also been theoretically studied [3, 61], has previously been proposed not only for theophylline derivatives but also for analogous molecules such as guanine and adenine.

For caffeine and theobromine, both with identical azole rings, the frontier orbitals are very similar and there is a LUMO character on N(9). Thus, an interaction with a rich metal center is also predicted. In fact, N(9) complexes of caffeine are well known [2, 60, 62–66], and there are examples reported with theobromine [3, 67–69]. The latter one also displays an acidic nature (LUMO) onto N(1), substituted by a proton. Some N(1) bounded species of theobromine have previously been reported [68].

As it can be seen from the HOMO-like orbitals in **1**-**3**, the bonding character in the oxo-substituted ring is similar to that of guanine or other purines [53]. It has been proposed that the reactivity of adenine and guanine might be due to stretching/twisting of the purine molecules due to delocalization of their bonding orbitals [53], which is easier in those than in the cases studied here. Molecules **1**-**3** are more constrained due to their planarity and, therefore, it is more difficult for those to adopt any twisted conformation in which their reactivity might be enhanced.

Synthesis of benzyl substituted imidazolium salts from methylated xanthines

The synthesis of imidazolium salts from methylated xanthines has only been reported for caffeine by different groups [10–13, 70]. However, only the methyl derivative has been synthesized. So far, to the best of our knowledge, there are no other examples of modified xanthines to produce imidazolium salts.

Our approach is based on the nucleophilic substitution of benzyl bromide by the methylated xanthines, as shown in Scheme 1. The reaction is straightforward and produces **1a**, **2a** and **3a** in moderate to good yields. This procedure has been previously used for the synthesis of a variety of imidazolium salts and ionic liquids [71, 72].

The new imidazolium salts **1a** and **3a** are soluble in common organic solvents such as chloroform or acetonitrile. The solubility of **2a** in most of the common organic

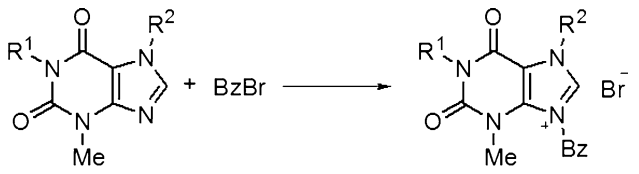

R^1 = Me; R^2 = H: (TheophyllineBz)Br (**1a**)
R^1 = H; R^2 = Me: (TheobromineBz)Br (**2a**)
R^1 = R^2 = Me: (CaffeineBz)Br (**3a**)

Scheme 1

solvents is poor, but better than its parent compound theobromine, **2**.

The new ligands were characterized using multinuclear NMR, FTIR and HRMS. As expected, all of the techniques indicate effective substitution on N(9). This becomes evident in the ^{1}H NMR spectra from the shift downfield of about 1 ppm observed in the –CH_2– protons of the benzyl group in all of the cases. This unshielding is indicative of the new N(9)–CH_2– bond formed. Also, H8 shifts in every case, compared to the parent compounds **1**–**3**. These data, along with the appearance of the carbonyl groups in the FTIR and the excellent match between the calculated and experimental values of HRMS confirms that we have indeed obtained the new imidazolium salts **1a**, **2a** and **3a**.

Interestingly, the nucleophyllic substitution was carried out over an aliphatic halide such as benzyl bromide. Even when there are some examples of this type of reaction for other imidazoles [71, 72], the previous example of modified xanthine, i.e. methyl caffeine, was obtained with very strong alkylating agents, such as dimethylsulphate or MeI [10–13, 70].

In fact, it is observed that the alkylation reaction occurs more easily on theophylline than on theobromine or caffeine. This observation could easily be explained by our theoretical studies, since, as it was explained before, it becomes obvious that the orbitals which interact with the alkylating agent are less available for caffeine than for theophylline or theobromine. As we have confirmed experimentally, the nucleophyllic substitution was only possible under harsh conditions: refluxing the xanthines in the neat alkylating agent (approximately 200 °C) for long periods of time (1–4 days).

On the other hand, when the synthesis of **1a** was attempted using strong reaction conditions, we also detected the dialkylated imidazolium salt (i.e. both N(9) and N(7) have been substituted by a benzyl group) as a minor reaction byproduct that could be characterized. The 1,3-dimethyl-9,7-dibenzylxanthinium bromide (tphBz_2Br, **1a**′) or other analog N(7) substituted species could be very interesting as potential carbene precursors, since a C(8) binding might be enhanced. This will be a matter of future communications.

Coordination chemistry of **1a**, **2a** and **3a** toward palladium

Methylated xanthines have previously been studied in coordination chemistry, and several examples are reported with the unmodified xanthines [5, 6, 8]. Also, some species resulting from the interaction between protonated species of theophylline, theobromine and caffeine and palladium-halide anions have been reported [3, 4], although these are not coordination compounds between the corresponding xanthine and palladium but plain electrostatic attractions.

Our main purpose was to obtain the NHC-Pd complex from our imidazolium salts **1a**, **2a** and **3a**. However, an interesting behavior was identified. One of the main problems in the stabilization of a carbenic species with theophylline is that one of the nitrogen atoms of the imidazole ring is substituted by a proton. Although there are examples in the literature in which Pd-NHC complexes with hydrogen substituting one of its nitrogen atoms have been obtained [9], some of those correspond to the product of an internal acid catalyzed reaction of a diamminopalladium (II) complex [73, 74].

When **1a** reacted with $Pd(OAc)_2$ [75–80], in an attempt to synthesize the Pd-NHC complex, a solvent dependant behavior was observed. A $CDCl_3$ solution of **1a** reacted in situ (NMR timescale) with $Pd(OAc)_2$, showed a shift in the signals (downfield) assigned to the ligand. A new signal attributed to H8 indicates that the interaction has occurred through N7 instead of C8. In another test, a DMSO-d_6 solution of the isolated compound (synthesized according to the procedure analogous to that of Huynh [81]) shows a low-field signal in the ^{13}C{^{1}H} NMR spectrum (δ 174), and the disappearance of the H8 proton in the ^{1}H NMR, both of them indicative of a carbenic interaction between **1a** and Pd(II). Interestingly, a septuplet observed in the ^{13}C{^{1}H} NMR spectrum is assigned to a DMSO ligand coordinated to Pd in this species, with a coupling constant of 19.6 Hz, which is similar to the values reported for this ligand in similar coordinative environments (J_{CD} = 21.0 Hz) [82].

Over time, the low-field signal in the ^{13}C{^{1}H} NMR spectrum shifts to higher fields and eventually disappears. In the ^{1}H NMR spectrum, as the very low field signal shifts, the signal corresponding to H8 is observed again. This behavior is indicative of a change in the coordination site toward Pd(II) and was also observed when the test was done using CD_3CN as solvent.

We propose an equilibrium between the carbene and the theophyllinate species, the kinetic product being the carbene and the thermodynamic product the theophyllinate, as depicted in Scheme 2. The dynamic behavior observed can

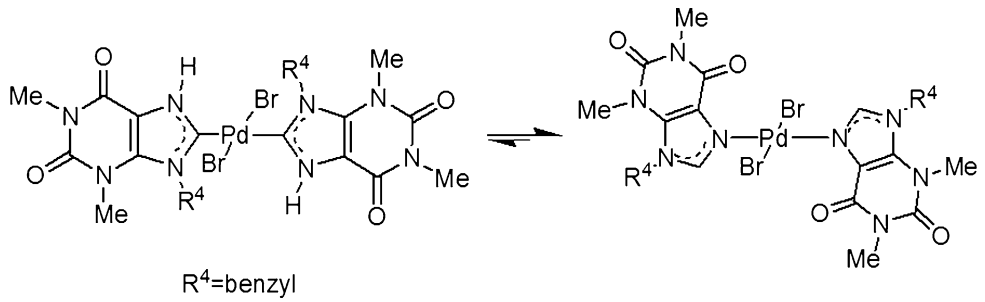

Scheme 2

be slowed with the solvent used. In fact, the "theophyllinate" species seems to be favored by poor coordinating solvents ($CDCl_3$, for example), since in those the carbenic species is almost undetectable. When the product is analyzed in strongly coordinating solvents such as DMSO-d_6, the carbene can be stabilized, and detected spectroscopically.

The behavior observed is possible, since the coordination of DMSO restrains the free rotation around the M-NHC complex due to its anisotropy [75–78]. In fact, in chloroform, the possibility of stabilizing the species through coordination of the solvent does not exist, and rotation becomes possible, explaining the double amount of signals observed on the NMR for the ligand in this complex (see Experimental section, synthesis of **4**). In this sense, in solution, the interconversion between the carbene and the N-coordinated species probably depends on the anisotropy of **1a** as NHC [75–78].

In an attempt to stabilize the carbene, the synthesis was repeated in acetonitrile using NaBr. Either with or without NaBr, the species obtained is the same, the N-coordination product, or "theophyllinate". The formation of the "theophyllinate" species is confirmed by X-ray diffraction and was either identified on NMR timescale and individually synthesized from $Pd(OAc)_2$ and **1a**. Figure 4 displays the solid state structure for $PdBr_2(tphBz\text{-}H)_2$, **4**. This complex is analogous to the previously reported $PdCl_2(tph)_2$ [6, 8] containing the unmodified theophylline ligand. Tables 1 and 2 show a summary of the crystal data and a selection of bond distances and angles respectively, for $PdBr_2(tphBz\text{-}H)_2$ (**4**).

Table 2 Selected bond distances (Å) and angles (°) for $PdBr_2(tphBz\text{-}H)_2$ (**4**)

Distances (Å)			
Pd1–N1^i	2.023(6)	Pd1–Br1^i	2.4261(11)
Pd1–N1	2.023(6)	Pd1–Br1	2.4261(11)
Angles (°)			
N1^i–Pd1–N1	180.000(2)	N1^i–Pd1–Br1^i	89.5(2)
N1^i–Pd1–Br1	90.5(2)	N1–Pd1–Br1^i	90.5(2)
N1–Pd1–Br1	89.5(2)	Br1–Pd1–Br1^i	180.0

The "i" atoms are generated by an improper S_2 axis, i.e., a reflection plus a rotation

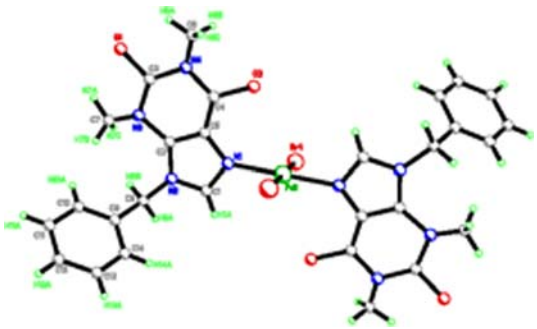

Fig. 4 Solid state structure of $PdBr_2(tphBz\text{-}H)_2$ (**4**)

Complex **4** crystallizes in a monoclinic system with a space group $P2_1/a$. As shown in Fig. 4, ligand **1a** is bounded to Pd through N(7) in an almost perfect square planar geometry, with a small deviation of 0.5° from the ideal 90° angle. In the solid state, the new "theophyllinate" complex **4** is absolutely co-planar, since both the Br1–Pd1–Br1^i and N1^i–Pd1–N1 angles are of 180 degrees, showing a high level of symmetry. The Pd–Br distance is 2.4261Å, typical length for this kind of bonds as reported previously for analogous species [81]. The Pd-N bond, 2.023Å, is also in the range of reported distances for Pd-Nsp^2 interactions [9]. The new "theophyllinate" complex is the trans isomer, probably in order to minimize the sterical hindrance between the xanthine ligands. In fact, this is also reflected in the transoid configuration adopted by the benzyl groups, with each one back and forward respectively in terms of the plane orthogonal to the one containing both of the nitrogen atoms in the $PdBr_2N_2$ unit. Regarding its spatial configuration and since the compound only presents one symmetry element, an improper S_2 axis, it can be classified as a C_i.

It has been observed that theophylline has a particular reactivity due to the presence of an acidic proton on the nitrogen [3, 9]. In most cases, theophylline coordinates as theophyllinate anionic species through this nitrogen [67]. For instance, Romerosa et al. have obtained a complex where both theophylline and 8-(methylthio)-theophylline are coordinated as monoanionic ligands to palladium (II) [9].

The interaction between theophylline and palladium complexes has previously been reported [63]. By reaction

of theophylline with K_2PdCl_4, two kinds of metallic complexes are formed, and either one depends on the acidity and the solvent used. Pneumatikakis et al. [63] identified two coordination modes for theophilline: the first one as a neutral ligand through N(9), obtaining K[Pd(theophylline)Cl_3], and the second one involving a monoanionic bidentate chelate through the N(7) and O(6), yielding a dimer such as [Pd(N^O-theophylline)Cl]$_2$ [63].

Then, the imidazolium salt **1a**, obtained from theophylline, acts mainly as an N-bounded ligand, confirming the nature of the binding site previously observed for the unmodified theophylline and other derivatives of it [9, 62, 63].

The theobromine derivative, **2a**, was also studied. One of the main problems with this one is that its poor solubility in most of the solvents makes it difficult to choose a reaction medium. Nevertheless, an in situ reaction was performed on the NMR timescale. Two sets of identical signals are observed in the ^{1}H NMR spectrum, in a 2:1 ratio, both of them shifted from those of **2a**. Interestingly, the acid proton assigned to N1-H is not observed. From the $^{13}C\{^1H\}$ NMR spectrum, it is possible to observe the signal corresponding to C8 basically at the same chemical shift from the parent compound **2a**, and no carbenic interactions are observed.

From these spectroscopic data, it is possible to propose a neutral coordination of **2a** to palladium through N1, with the general formula of $PdBr_2$(tbrBz-H)$_2$. With the information available, it is not possible to assign a specific spatial configuration of the isomers or which isomer is the major one. The structures proposed for these species are shown in Fig. 5. This reaction is currently being scaled up, and further studies on the characteristics of these species will be performed.

There are some examples of N-coordinated complexes from the unmodified theobromine in the literature [63]. However, in those examples theobromine coordinated as a monoanionic ligand to palladium and platinum. To the best of our knowledge, this is the first example of an imidazolium salt with theobromine, and as a consequence, the first coordination compound reported of it.

Since both the theophylline and the theobromine benzyl derivatives tend to interact with palladium as N-coordinated species, but in the case of **1a** it was possible to detect a carbenic species, it becomes interesting to contrast these ligands with the analogous 1,3,7-trimethyl-9-benzylxanthinium bromide (**3a**) in which the possibility of N-coordination is blocked, since N1, N3 and N7 are substituted by methyl groups.

The coordination study of CaffBzBr (**3a**) was initially performed in situ on the NMR timescale. A reaction between $Pd(OAc)_2$ and **3a** in $CDCl_3$ was studied, observing that the ligand does not react completely, but a clear set of shifted signals lacking the one assigned to H8 appears in the ^{1}H NMR. The species is stable even after 24 h. However, even when this behavior was observed, the amount of ligand that reacts under the same conditions when the reaction is scaled up is negligible, and very low yields of the carbene are obtained and the unreacted ligand is recovered almost completely. This might be a consequence of the strength of the acetate, which acts as an internal base and should deprotonate C8 to generate the free carbene.

In the case of **3a**, the use of a stronger base to deprotonate C8 is possible, since the only acidic proton in the ligand is H8, and no further modifications of the chemical structure would occur, as in **1a** or **2a**. Using KO^{t}Bu as deprotonating agent, and $PdCl_2(NCPh)_2$ as palladium precursor, it was possible to obtain the Pd-NHC complex from **3a**, in good yields (86%). The pale yellow product was characterized using multinuclear NMR. The ^{1}H NMR spectrum lacks the signal assigned to H8, and all of the other signals shift downfield. Based on these results, it is possible to propose a

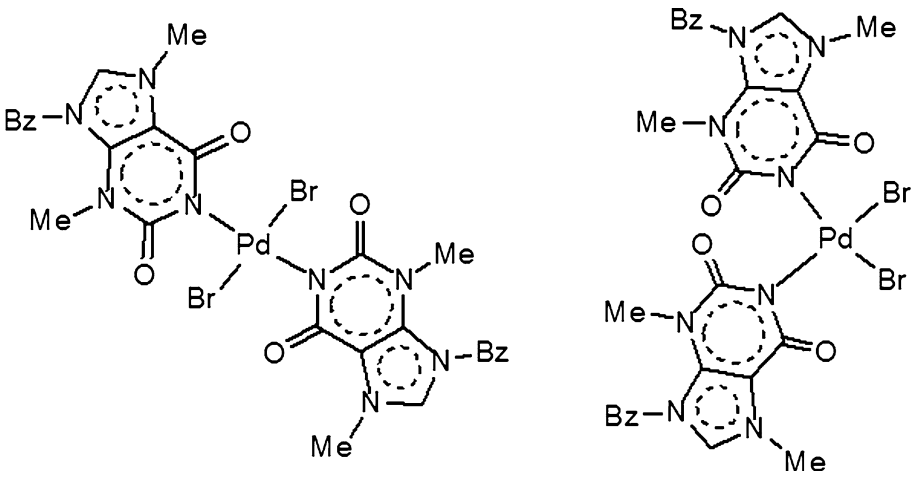

Fig. 5 Proposed structures for the N-coordinated product $PdBr_2$(tbrBz-H)$_2$ (**5**)

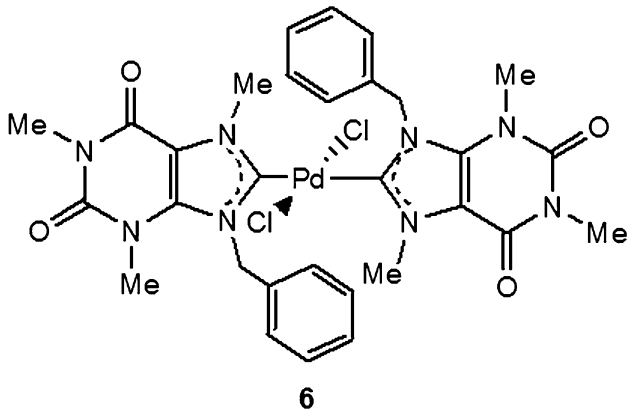

Fig. 6 Proposed structure for $PdCl_2(CaffBz)_2$ (**6**)

biscarbene complex, such as $PdCl_2(caffBz)_2$ (**6**) (Fig. 6). Steric hindrance might become the driving force for the proposed configuration. The available information does not provide further evidence to assign a final stereochemistry. However, the proposed configuration is based on the previous examples [13] of NHC's from methylated caffeine, an imidazolium salt analogous to **3a**.

Conclusions

Three new imidazolium salts based on natural methylated xanthines bearing the benzyl group onto N(9) were synthesized and characterized. The coordination chemistry toward palladium of these potential NHC's precursors was studied. **1a** acts both as a carbenic and an N-bounded ligand, in a behavior strongly dependent on the coordinative properties of the reaction media. An equilibrium is proposed between both species, the carbene being the kinetic product, while the N-coordination is favored by the thermodynamics. **2a** acts essentially as an N-bounded ligand, and the C(8) coordination was not detected spectroscopically, and a mixture of isomers is proposed. Finally, **3a** is bounded to palladium as expected, as an NHC, i.e., via C(8), since in this case there are no other potential coordination sites.

The two theoretical models described for **1**, **2** and **3**, agree completely with our synthetic experiences and with the experimental facts previously reported. Both approaches could be valuable tools in future xanthines' chemistry studies, to predict reactivities and trends based on acid–base considerations. In fact, the synthesis of other imidazolium salts from methylated xanthines and their complexes is currently under study and will be matter of a future communication.

Acknowledgments The authors thank the Decanato de Investigación y Desarrollo de la Universidad Simón Bolívar (DID-USB) for promoting this scientific activity, and Laboratorios FARMA (Caracas, Venezuela) for a generous loan on theophylline. We also thank ETH Zürich DCHAB/LOC MS-Service for performing the HRMS analyses and Lic. Giuseppe Lubes for some previous synthetic tests.

References

1. Lusty JR, Lee PF (1984) Inorg Chim Acta 91:L47–L49
2. Goodgame DML, Hayman PB, Riley RT, Williams DJ (1984) Inorg Chim Acta 91:89–93
3. Colacio-Rodríguez E, Salas-Peregrin JM (1984) Thermochim Acta 74:45–54
4. Moreno-Vida MI, Colacio-Rodríguez E, Moreno-Carretero MN, Salas-Peregrin JM, Simard M, Beauchamp AL (1989) Inorg Chim Acta 157:201–207
5. Moreno-Vida MI, Colacio-Rodríguez E, Moreno-Carretero MN, Ruiz-Sánchez J, Salas-Peregrin JM (1987) Thermochim Acta 115:45–55
6. Salas-Peregrin JM, Colacio-Rodríguez E, Romero-Molina MA, Sánchez-Sánchez MP (1983) Thermochim Acta 69:313–321
7. Clarke MJ, Taube H (1975) J Am Chem Soc 97:1397–1403
8. Umapathy P, Harnesswala RA, Dorai CS (1985) Polyhedron 4:1595–1602
9. Romerosa A, Varela JS, Hidalgo MA, Avila-Rosón JC, Colacio E (1997) Inorg Chem 36:3784–3786
10. Kascatan-Nebioglu A, Panzner MJ, Garrison JC, Tessier CA, Youngs WJ (2004) Organometallics 23:1928–1931
11. Kascatan-Nebioglu A, Melaiye A, Hindi K, Durmus S, Panzner MJ, Hogue LA, Mallett RJ, Hovis CE, Coughenour MH, Crosby SD, Milsted A, Ely DL, Tessier CA, Cannon CL, Youngs WJ (2006) J Med Chem 49:6811–6818
12. Melaiye A, Simons RS, Milsted A, Pingitore F, Wesdemiotis C, Tessier CA, Youngs WJ (2004) J Med Chem 47:973–977
13. Herrmann WA, Schütz J (2004) J Organomet Chem 689:2995–2999
14. Chung CK, Grubbs RH (2008) Org Lett 10:2693–2696
15. Poyatos M, McNamara W, Incarvito C, Clot E, Peris E, Crabtree RH (2008) Organometallics 27:2128–2136
16. Ray L, Shaikh MM, Ghosh P (2008) Inorg Chem 47:230–240
17. Radius U, Bickelhaupt FM (2009) Coord Chem Rev 253:678–686
18. Jacobsen H, Correa A, Poater A, Costabile C, Cavallo L (2009) Coord Chem Rev 253:687–703
19. Buscemi G, Biffis A, Tubaro C, Basato M (2009) Catal Today 140:84–89
20. Beck W, Kottmair N (1976) Chem Ber 109:970–993
21. Herrmann WA (2002) Angew Chem Int Ed 41:1290–1309
22. Doyle JR, Slade PE, Jonassen HB (1960) Inorg Synth 6:216–219
23. North ACT, Phillips DC, Mathews FS (1968) Acta Cryst A. 24:351–359
24. Sheldrick GM, SHELX-97 (Release 97-2) (1997) Program for structure refinement. University of Gottingen, Gottingen
25. Leboeuf M, Koster M, Jug K, Salahub DR (1999) J Chem Phys 111:4893–4905
26. Gadre SR, Shirsat RN (2000) Electrostatics of atoms and molecules. Universities Press, Hyderabad
27. Pingale SS, Gadre SR, Batolotti LJ (1998) J Phys Chem A 102:9987–9992
28. Deshmukh MM, Sastry NV, Gadre SR (2004) J Chem Phys 121:12402–12410
29. Joshi KA, Gejji SP (2005) J Mol Struc Theochem 724:87–93
30. Tachikawa H, Iyama T, Kawabata H (2005) J Mol Struc Theochem 718:117–122
31. Pathak RK, Gadre SR (1990) J Chem Phys 93:1770–1773

32. Gadre SR, Kulkarni SA, Shrivastava IH (1992) J Chem Phys 96:5253–5260
33. Gadre SR, Pathak RK (1989) Proc Ind Acad Sci (Chem Sci) 102:189–192
34. Alhambra C, Luque FJ, Orozco M (1995) J Phys Chem 99:3084–3092
35. Kornelak P, Michalak A, Najbar M (2005) Catal Today 101:175–183
36. Michalak A (2004) Chem Phys Lett 386:346–350
37. Politzer P, Truhlar DG (1982) Chemical applications of atomic and molecular electrostatic potentials. New York, Plenum
38. Murray JS, Sen KD (1996) Molecular electrostatic potential: concepts and applications. Elsevier, Amsterdam
39. Orozco M, Luque FJ (1996) Theor comput Chem Ser 3:181
40. Aray Y, Marquez M, Rodríguez J, Coll S, Simón-Manso Y, Gonzalez C, Weitz DA (2003) J Phys Chem B 107:8946–8952
41. Aray Y, Marquez M, Rodríguez J, Coll S, Simón-Manso Y, Gonzalez C, Weitz DA (2004) J Phys Chem B 108:2418–2424
42. Aray Y, Rodríguez J, Coll S, Gonzalez C, Marquez M (2004) J Phys Chem B 108:18942–18948
43. Tal Y, Bader RFW, Erkku J (1980) Phys Rev A 21:1–11
44. Keith TA, Bader RFW, Aray Y (1996) Int J Quantum Chem 57:183–198
45. Sjoberg P, Politzer P (1990) J Phys Chem 94:3959–3961
46. Aray Y, Rodríguez J (2007) J Mol Catal A 265:32–41
47. Aray Y, RodrÍguez J, Vega D (2006) In: Matta CF, Boyd RJ (eds) The quantum theory of atoms in molecules: from DNA to solid and drug design. Wiley-VCH, Weinheim
48. Aray Y, Rodríguez J, Coll S, Rodríguez-Arias E, Vega D (2005) J. Phys. Chem. B 109:23564–23570
49. Delley B (1990) J Chem Phys 92:508
50. Delley B (2000) J Chem Phys 113:7756
51. Perdew JP, Wang Y (1992) Phys Rev B 45:13244–13249
52. Chen J, Chen L, Xu L, Zheng K, Ji L (2008) J Phys Chem B 112:9966–9974
53. Serrano-Andrés L, Merchán M, Borin AC (2008) J Am Chem Soc 130:2473–2484
54. Ramaekers R, Dkhissi A, Adamowicz L, Maes G (2002) J Phys Chem A 106:4502–4512
55. Major DT, Laxer A, Fischer B (2002) J Org Chem 67:790–802
56. Virta P, Koch A, Roslund MU, Mattjus P, Kleinpeter E, Kronberg L, Sjöholm R, Klika KD (2005) Org Biomol Chem 3:2924–2929
57. Gonella NC, Roberts JD (1982) J Am Chem Soc 104:3162–3164
58. Dutta Saikia M, Dutta NN (2006) Col Surfa A 280:163–168
59. Huang Y, Kenttamaa H (2004) J Phys Chem A 108:4485–4490
60. Blanco F, Alkorta I, Zborowski K, Elguero J (2007) Struct Chem 18:965–975
61. Baik M, Friesner RA, Lippard SJ (2003) J Am Chem Soc 125:14082–14092
62. Pneumatikakis G (1984) Inorg Chim Acta 93:5–11
63. Pneumatikakis G, Yannopoulos A, Markopoulos J, Angelopoulos C (1988) Inorg Chim Acta 152:101–106
64. Rajendran S, Amalraj AJ, Joice MJ, Anthony N, Trivedi DC, Sundaravadivelu M (2004) Corr Rev 22:233–248
65. Kolaylı S, Ocak M, Küçük M, Abbasoğlu R (2004) Food Chem 84:383–388
66. Nafisi S, Sadjadi AS, Zadeh SS, Damerchelli M (2003) Biomol Struct & Dynam 21:289–296
67. Mikulski CM, Kurlan MK, Bayne M, Gaul M, Karayannis NM (1988) J Coord Chem 17:267–275
68. Mikulski CM, Grossman S, Lee CJ, Karayannis NM (1987) Trans Met Chem 12:21–25
69. Mikulski CM, Grossman S, Bayne ML, Gaul M, Kanach D, Udell K, Karayannis NM (1990) Inorg Chim Acta 173:31–35
70. Ivanov EI, Kalayanov GD, Yaroshchenko IM, Stepanov DE (1989) Chem Heterocyc Comp 25:1318
71. Dupont J, Consorti CS, Suarez PAZ, de Souza RF (2004) Org Synth 10:184–187
72. Creary X, Willis E (2005) Org Synth 82:166–167
73. Ito Y, Hirao T, Tsubata K, Saegusa T (1978) Tetrahedron Lett 18:1535–1538
74. Fehlhammer WP, Bliβ T, Fuchs J, Holzmann G (1992) Zeitschrift Fur Naturforschung. 47B:79–89
75. Glorius F (2007) Top Organomet Chem 21:1–20
76. Díez-González S, Nolan SP (2007) Top Organomet Chem 21:47–82
77. Peris E (2007) Top Organomet Chem 21:83–116
78. Tekavec TN, Louie J (2007) Top Organomet Chem 21:159–192
79. Herrmann WA, Schwarz J, Gardiner MG, Spiegler M (1999) J Organomet Chem 575:80–86
80. Loch JA, Albrecht M, Peris E, Mata J, Faller JW, Crabtree RH (2002) Organometallics 21:700–706
81. Huynh HV, Han Y, Ho JHH, Tan GK (2006) Organometallics 25:3267–3274
82. Gottleib HE, Kotlyar V, Nudelman A (1997) J Org Chem 62:7512–7515